Journal of the Korean Society of Marine Engineering, Vol.30, No.4, pp.494~504, 2006(ISSN 1226-9549)

A Modified Two-Parameter Solution for Crack-Tip Field in Bending Dominated Specimens

Seok-Ki Jang† · Xian-Kui Zhu**

(Manuscript : Received FEB 28, 2006 ; Revised MAY 23, 2006)

Abstract : It is well known that the two-parameter $J-A_2$ solution can well characterize the crack-tip fields and quantify the crack-tip constraint for different flawed geometries in variety of loading conditions. However, this solution fails to do so for bending dominated specimens or geometries at large deformation because of the influence of significant global bending stress on the crack-tip field. To solve this issue, a modified $J-A_2$ solution is developed in this paper by introducing an additional term to address the global bending influence. Using the J_2 flow theory of plasticity and within the small-strain framework, detailed finite element analyses are carried out for the single edge notched bend (SENB) specimen with a deep crack in A533B steel at different deformation levels ranging from small-scale yielding to large-scale yielding conditions. The numerical results of the crack-tip stress field are then compared with those determined from the $J-A_2$ solution and from the modified $J-A_2$ solution at the same level of applied loading. Results indicate that the modified $J-A_2$ solution largely improves the $J-A_2$ solution, and match very well with the numerical results in the region of interest at all deformation levels. Therefore, the proposed solution can effectively describe the crack-tip field and the constraint for bending dominated specimens or geometries.

Key words : Crack-tip field, constraint, $J-A_2$ solution, bending specimen, large-scale yielding

1. Introduction

The single-parameter fracture criterion based on the J-integral[1] and the HRR singularity field[2),(3)] has been extensively investigated and applied in integrity assessments of flawed structures. However, it is well known that the fracture constraint at the crack tip has significant effects on the crack-tip fields and the fracture toughness of materials[4)-(6)]. It is commonly accepted that the Hutchinson-Rice-Rosengren(HRR) field can provide an effective characterization of the crack-

† Corresponding Author(Dept. of Marine Engineering, Mokpo Maritime University)
E-mail : jangsk @ mmu.ac.kr, Tel : 061) 240-7093
* Battelle, Columbus, Ohio 43221, U.S.A.

tip field only for high constraint specimens, but can not for low constraint specimens due to the constrain effect on the crack-tip field. Consequently, several fracture constraint theories for the low constraint specimens have been developed, typically including the J-T approach[7],[8], the J-Q theory[9],[10] and the $J-A_2$ three-term solution[11],[12].

A more detailed reviews of investigations on fracture constraints and the two-parameter crack-tip fields were reported in Chao and Zhu[13], who also presented the size requirements of a two-parameter fracture criterion based the $J-A_2$ solution. Jang and Zhu[4] then extended the $J-A_2$ two-parameter characterization for quantifying crack-tip constraint effect on the fracture resistance curves (i.e. J-R curves) for ductile crack growth. Similar work was done by Zhu and Jang[5] using the J-Q theory. Due to the global bending influence, both the single-parameter and two-parameter crack-tip solutions are valid for small-scale yielding (SSY) conditions to correctly describe the crack-tip field of bending specimens, such as the single edge notched bend (SENB), single edge notched tension (SENT) and compact tension (CT) specimens. It has been extensively found that the three fracture constraint theories cannot correctly characterize the crack-tip field for these bending dominated specimens: SENB, SENT and CT under large-scale yielding (LSY) or fully plastic deformation. Investigators involving researches on this topic include Shih and German[14], O'Dowd and Shih[10], Parks[15], Wang and Parks[16], Wei and Wang[17], Karstensen et al.[18], and Lam et al.[19]. Accordingly, none of the available crack-tip solutions can be correctly used to characterize the crack-tip field for bending dominated specimens within the crack-tip region prone to ductile fracture.

So motivated, this paper focuses on the $J-A_2$ three-term solution and develops a modification for the $J-A_2$solution by introducing an additional term to address the global bending influence and to characterize the crack-tip stress field of deeply cracked SENB specimens under LSY conditions. In the modified $J-A_2$ four-term solution, J still represents the intensity of applied loads, A2still describes the crack-tip constraint level, and the third new parameter is the global bending moment directly related to the applied load. Comparison with detailed finite element results shows that the modified $J-A_2$solution agrees well with the full-field solutions. Therefore, the proposed solution can accurately describe the crack-tip field and the corresponding parameter A_2 can effectively quantify the constraint level of bending dominated specimens for both LSY and SSY.

2. The $J-A_2$ asymptotic solution and its modification

Chao and Zhu[13] have shown that the two-parameter J-A2three-term solution is valid to characterize the crack-tip field only within a small fraction of the ligament. For the SENB specimen, the influence of global bending on the crack-tip field is very small within the valid

region, but becomes large gradually beyond that region. To accurately characterize the crack-tip stress field and constraint of bending dominated specimens under LSY conditions, the modified $J-A_2$ solution is developed next.

2.1 The $J-A_2$ three-term solution

To efficiently characterize the crack-tip field and quantify constraint effect, Yang et al.[11] and Chao et al.[12] developed the $J-A_2$ three-term solution with J-integral as the applied load intensity and A_2 being the constraint parameter. Under plane strain conditions, the three-term asymptotic stress field can be expressed as

$$\frac{\sigma_{ij}}{\sigma_o}=A_1\left[\left(\frac{r}{L}\right)^{s_1}\widetilde{\sigma_{ij}^{(1)}}(\theta)+A_2\left(\frac{r}{L}\right)^{s_2}\widetilde{\sigma_{ij}^{(2)}}(\theta)+A_2^2\left(\frac{r}{L}\right)^{s_3}\widetilde{\sigma_{ij}^{(3)}}(\theta)\right] \tag{1}$$

where the stress angular functions $\widetilde{\sigma_{ij}^{(k)}}(\theta)$ $(k=1, 2, 3)$ where the stress angular functions $s_k\,(s_1, s_2, s_3)$ depend only on the strain hardening exponent n, and are independent of the other material constants (i.e. hardening parameter α, yield stress σ_o and yield strain $\epsilon_o=\sigma_o/E$) and the applied load. When the strain hardening exponent $n\geq 3$, the three stress exponents are not independent, and related by $s_3=2s_2-s_1$. The values of $\tilde{\sigma}_{ij}^{(k)}(\theta)$ and s_k are tabled in Chao and Zhang[20]. L is a characteristic length parameter and L = 1 mm has been taken in this work. The parameters A_1 and s_1 have the same expressions as given in the HRR singularity field:

$$A_1=\left(\frac{J}{\alpha\epsilon_o\sigma_o I_n L}\right)^{-s_1},\quad s_1=-\frac{1}{n+1} \tag{2}$$

The parameter A_2 is a measurement of crack-tip constraint level. Using the point matching method, one can determine the value of the parameter A_2 by matching the crack-opening stress from the $J-A_2$ solution with the finite element analyses(FEA) result at $r/(J/\sigma_o)=1\sim 2$, for example.

2.2 A modification of the $J-A_2$ solution

As mentioned in Introduction, the $J-A_2$ three-term solution can not accurately characterize the crack-tip field for deeply cracked bending specimens under LSY or fully plastic deformation, and thus it has to be modified for such a purpose. For elastic-plastic crack problems, the applied bending stress is independent of the crack-opening stress, but inversely the opening stress depends on the applied bending stress. Since both the opening and bending stresses on the ligament are partly nonlinear under LSY conditions, it is too hard to accurately consider the global bending stress in the asymptotic crack-tip field. As an approximation, however, it is assumed here that the opening stress (noted it is referred to as $\sigma_{\theta\theta}$ at $\theta=0^o$ hereafter) for bending specimens is a simple superposition of the $J-A_2$ solution, $\sigma_{\theta\theta}^{JA_2}$ and the global bending stress, $\sigma_{\theta\theta}^{M}$:

$$\sigma_{\theta\theta}=\sigma_{\theta\theta}^{JA_2}+\sigma_{\theta\theta}^{M}, \tag{3}$$

Extensive finite element analyses, as

reported by O'Dowd and Shih[10], Wang and Parks[16], Wei and Wang[17], Karstensen et al.[18], Chao and Zhu[13] and the present work, indicate that the global bending stress dominates the crack-tip stress field for bending specimens under LSY conditions so that the opening stress linearly distributes on the ligament away from the crack tip even within the interest region of $1<r/(J/\sigma_o)<5$. Motivated by the linearly elastic stress distribution on the ligament from the strength of materials theory, it is assumed in this work that the global bending stress $\sigma_{\theta\theta}^{M}$ in Eq. (3) is a linear function of the distance from the crack tip, r, and the global bending moment, M about the ligament plane of specimens:

$$\sigma_{\theta\theta}^{M}(\theta=0)=C\frac{Mr}{b^3} \tag{4}$$

where C is an undetermined load-independent constant, and M is the moment per unit length. The ligament length b is arbitrarily inserted in Eq. (4) so that the C is a non-dimensional constant. In Eq. (4), the plane strain conditions are assumed, and the thickness is taken as unity, i.e. $B=1mm$.

Substituting Eqs (1) and (4) into Eq. (3), we obtain the general form of the modified J-A_2 solution for the opening stress ahead of the crack tip, i.e.$\theta=0^o$, as follows:

$$\frac{\sigma_{ij}(0)}{\sigma_o}=A_1\left[\left(\frac{r}{L}\right)^{s_1}\widetilde{\sigma_{\theta\theta}^{(1)}}(0)+A_2\left(\frac{r}{L}\right)^{s_2}\widetilde{\sigma_{\theta\theta}^{(2)}}(0)+A_2^2\left(\frac{r}{L}\right)^{s_3}\widetilde{\sigma_{\theta\theta}^{(3)}}(0)\right]+\frac{CMr}{\sigma_o b^3} \tag{5}$$

Our detailed finite element analysis as presented later indicates the constant $C\approx-6$. From (3), therefore, the constraint parameter A_2 can be determined at $r/(J/\sigma_o)=1\sim2$, for example, by solving the following equation:

$$A_2^2\left(\frac{r}{L}\right)^{s_3}\widetilde{\sigma_{yy}^{(3)}}(0)+A_2\left(\frac{r}{L}\right)^{s_2}\widetilde{\sigma_{yy}^{(2)}}(0)+A_1\left(\frac{r}{L}\right)^{s_1}\widetilde{\sigma_{yy}^{(1)}}(0)-\frac{6Mr}{\sigma_o b^3 A_1}-\frac{\sigma_{yy}^{FEA}(0)}{\sigma_o A_1}=0 \tag{6}$$

where both J (and thus A_1) and $\sigma_{\theta\theta}^{FEA}(0)$ are obtained from the FEA calculations, and M is the resulting applied moment at the cross section of crack plane in bending specimens.

The modified $J-A_2$ solution is simply referred to be as the $J-A_2-M$ solution hereafter. It has three "parameters", A_1, A_2 and M. However, both (or J, see (2)) and Mare related to the applied load. As a result, the $J-A_2-M$ four-term solution simply incorporates the global bending stress, but does not really introduce any new parameter in the asymptotic solution. The two parameters remain as the applied loading (J and M) and the constraint level (A_2). The numerical results reported later will demonstrate the efficiency of the $J-A_2-M$ solution to characterize the crack-tip fields and quantify constraint levels for deeply cracked bending specimens under the LSY conditions.

3. Finite element modeling

To demonstrate the global bending effect on the crack tip stress field in deeply cracked bending specimens under

LSY and validate the present model, detailed plane strain finite element analyses (FEA) have been performed for the SENB specimen with a deep crack in ductile materials with different material hardening properties. Specimen geometry, material response and FEA model are described as below, and full-field FEA results will be reported in next section.

3.1 Specimen geometry

The most commonly used bending specimen, i.e. SENB is considered in this work and illustrated in Fig. 1(a). The specimen width is W=50mm, the crack length a=37.5mm, the remaining ligament b=12.5mm, the span S=4W, and the specimen length L=1.2S. Accordingly, the ratio of the crack depth to the specimen width is a/W=0.75, which shows that this SENB specimen is a deeply cracked specimen with high constraint.

3.2 Material response

Material considered in this work is A533B steel. This steel is commonly used in nuclear pressure vessels. For the A533B steel, the material constants are the yield stress $\sigma_o = 450MPa$, the yield strain $\epsilon_o = 0.002$, the Poisson's ratio $\nu = 0.3$, the hardening parameter $\alpha = 3/7$. Two hardening exponents $n = 3$ and 10 are considered to typically represent the high and low hardening materials, and to examine the influence of strain hardening exponents on the crack-tip field simulations.

Plastic deformation behavior of materials is modeled using the deformation theory of plasticity within the framework of the small strain theory, since this plasticity theory is simple and effective for elastic-plastic crack problems under all deformation levels. The constitutive response of the material obeys the power-law hardening stress-strain relation, which can be expressed as the following three-dimensional constitutive equation:

$$\frac{\epsilon_{ij}}{\epsilon_0} = (1+\nu)\frac{\sigma_{ij}}{\sigma_0} - \nu\frac{\sigma_{kk}}{\sigma_0}\delta_{ij} + \frac{3}{2}\left(\frac{\sigma_e}{\sigma_0}\right)^{n-1}\frac{s_{ij}}{\sigma_0} \qquad (7)$$

where $\sigma_0$is the initial yield stress, $\epsilon_0$is the yield strain and $\sigma_0 = E\epsilon_0$ with E as the Young's modulus, ν is the Poisson ratio, n is the strain hardening exponent, α is a material hardening constant; $s_{ij} = \sigma_{ij} - \sigma_{kk}\delta_{ij}/3$ are the deviatoric stress components; and $\sigma_e = (2s_{ij}s_{ij}/3)^{1/2}$ is the Mises effective stress.

3.3 Finite element model

Due to symmetry, only one half of the SENB specimen was modeled. The FEA mesh for this specimen is illustrated in Fig. 1(b). The finest mesh was generated at the crack tip, and the coarse mesh somewhere else. The smallest element size at the crack tip is 3.45×10^{-3}mm.

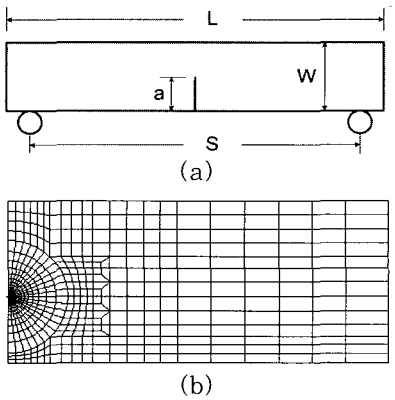

Fig. 1 Single edge notched bend [SENB] specimen for analysis.(a)specimen, (b)finite element mesh

Total 945 eight-node plane strain, isoparametric elements with reduced integration and 2976 nodes were used in this FEA model. The variety of geometry and loading configurations were generated by applying different crack sizes, kinematic boundary and loading conditions. When a/W= 0.75, the specimen was loaded by a couple of bending moments at the two ends. The support and symmetric boundary conditions were employed in this model. All FEA calculations were conducted using the commercial FEA code ABAQUS (version 6.4). Detailed FEA results are analyzed in the following sections.

4. Numerical results and analyses

4.1 Low hardening material with n=10

The FEA calculations were first performed for the SENB specimen with a/W = 0.75 in a low hardening material of $n=10$ under different loading. The objective is further to demonstrate influences of the global bending on the crack-tip field in the A533B steel, and validate the modified $J-A_2$ four-term solution for describing such problems by comparing to FEA results.

4.1.1 Full-field numerical results.

Four different loading levels, i.e. $b\sigma_0/J=$ 600, 200, 60, and 30 are selected in the FEA calculations for the SENB specimen in the A533B steel to cover various deformation levels ranging from SSY to LSY. Fig. 2(a) plots the radial distribution of the opening stress along the ligament near the crack tip for the four deformation levels of $b\sigma_0/J=$ 600, 200, 60, and 30. This figure shows that the opening stress increases as the loading increases in the tensile region ahead of the crack tip. The distribution of the opening stress over the distance from the crack tip is nonlinear at small load, but becomes linear gradually at large load except for the vicinity very close to the crack tip. Therefore, it is evident that the linear portion of the opening tensile stress on the ligament increases as the loading increases.

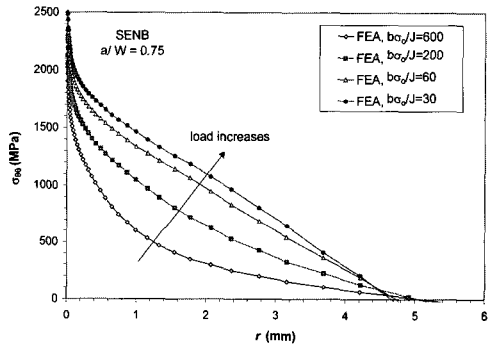

(a)

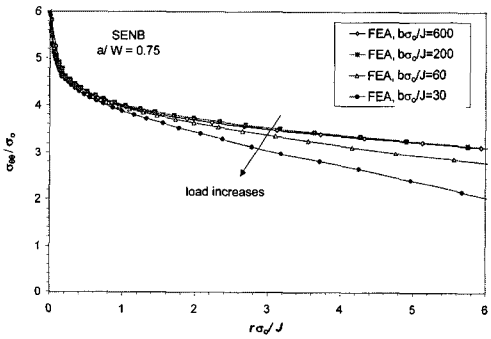

(b)

Fig. 2 Radial distribution of numerical opening stress for SENB specimen under the four loading cases. (a) real sizes, (b)normalized sizes

Fig. 2(b) shows the distributions of the normalized opening stress, $\sigma_{\theta\theta}/\sigma_0$ as a function of the normalized radial distance, $r/(J/\sigma_0)$ for the same four loading cases.

It is clear that using these axis scales the crack-tip opening stress decreases with increasing applied loads, as reversed distributions of real opening stress versus real radial distance. Moreover, the opening stresses are almost identical to each other for the two SSY loads of $b\sigma_0/J=600$ and 200. However for loading levels at LSY, i.e. $b\sigma_0/J \leq 60$, the opening stress gradually deviates from the results of $b\sigma_0/J=200$, and shows a strong linear distribution within the region of interest. This further demonstrates that the global bending stress significantly impinges the crack-tip stress field in the region of interest.

4.1.2 Determination of the constraint parameter A_2.

Using the FEA results of the opening stress on the ligament at $r/(J/\sigma_0)=1\sim 2$, the values of A_2 are determined using Eq. (6). For the four loading cases, i.e. $b\sigma_0/J=600$, 200, 60 and 30, the applied moment M are given for SENB specimen as 16328, 24971, 31560 and 34431 $N\cdot m$. The corresponding J-integrals are obtained from FEA as 9.27, 27.81, 92.71 and 185.40 KJ/m^2, and then the A_2 values are determined as 0.218, 0.222, 0.165, and 0.165, respectively. It is noted that for each loading the constraint parameter A_2 is a distance-independent constant, and thus the two-point matching method is used to determine the constant C and the constant $C=-6$ for these deformation.

4.1.3 Stress field under large-scale yielding

Since the $J-A_2$ solution can well describe the crack-tip stress field for the deeply cracked bending specimens under SSY conditions, the stress fields discussed for the SENB specimen are focused on for the one LSY loading, and also for the two contained yielding loads. Figures 3(a) to 3(c) show the distributions of the opening stress determined from FEA, the $J-A_2$ solution and the solution along the ligament for the three loading cases, $b\sigma_0/J=200$, 60 and 30, respectively, where the values of A2 are 0.222 for the smallest loading, and 0.165 for other two loadings. The results in Fig. 3 indicate that (1) the $J-A_2-M$ solution can match well with the FEA numerical results within the region of interest under all loading levels; (2) the $J-A_2$ solution also matches well with the FEA results for the containing yielding loading, i.e. $b\sigma_0/J\approx 60$, but then deviates gradually from the numerical results in the region of interest at the LSY loading of $b\sigma_0/J=30$; and (3) both asymptotic solution dominance zones reduce to $r\sigma_0/J<15$. Under LSY deformation, the zone of $J-A_2-M$ dominance is at least up to $r\sigma_0/J\approx 5$, while the zone of $J-A_2$ dominance is only up to $r\sigma_0/J\approx 2$. As a result, one can conclude that the modified $J-A_2$ solution has large enough dominance zone to cover the region of interest, $1\leq r\sigma_0/J\leq 5$, and can well characterize the crack-tip field of bending specimen under the LSY conditions for the hardening materials considered in this work.

In the discussion above, we have focused our attention on the opening stress. Similar trends can be found if the

comparisons are made by using other stress components. It is noted that the different scales of the horizontal coordinate $r/(J/\sigma_0)$ in Fig. 3 actually correspond to the same actual distance r from the crack tip under the three different levels of deformation. Similar scale rules were utilized in Fig. 4 in next sections.

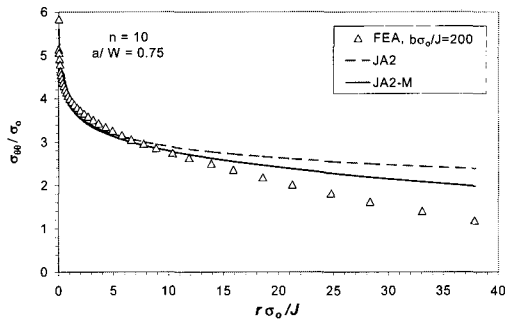

(a)

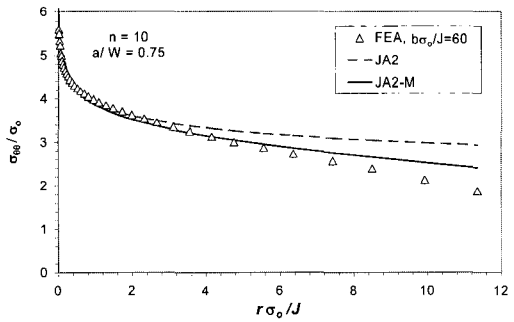

(b)

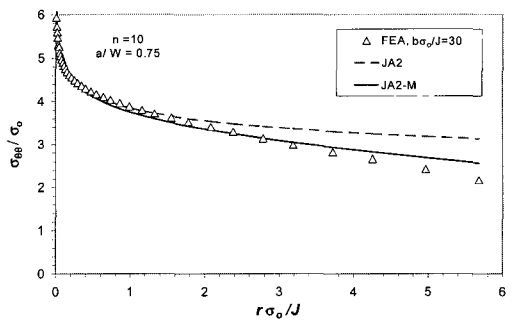

(c)

Fig. 3 Distribution of the opening stress along the ligament from FEA results and the asymptotic solution for the specimen with a/W=0.75 and n=10. (a)$b\sigma_o/J=200$, (b)$b\sigma_o/J=60$, (c)$b\sigma_o/J=30$

4.2 High hardening material with n=3

Similar FEA calculations were carried out in this section for the SENB specimen with a/W=0.75 in a high hardening material of$n=3$. Three different loading levels, i.e. $b\sigma_0/J=200$, 60, and 30 were also selected in the FEA calculations to cover the deformation varying from the SSY to LSY. The objective is to check the influence of the global bending on the crack-tip field and the size of $J-A_2$ or $J-A_2-M$ dominance zone for the high hardening material.

The distributions of the opening stress obtained from FEA, the $J-A_2$ solution and the $J-A_2-M$ solution along the remaining ligament are shown in Figs 4(a) to 4(c) for the three loading cases, $b\sigma_0/J=200$, 60 and 30, respectively. The corresponding values of A_2 used in the asymptotic solutions in Fig. 4 are -0.675, -0.593, -0.488.

The results in Fig. 4 indicate that (1) the $J-A_2-M$ solution agrees well with the FEA numerical results within the region of interest under all loading levels; (2) the $J-A_2$ solution also matches well with the FEA results for the containing yielding loading, i.e. $b\sigma_0/J\approx60$, but deviates gradually from the numerical results in the region of interest at the LSY loading of $b\sigma_0/J=30$; and (3) the size of $J-A_2-M$ dominance zone is $b\sigma_0/J\approx60$, 18 and 9, respectively for the three loading, while the $J-A_2$ valid zone shrinks from $b\sigma_0/J\approx50$ at the SSY loading of $b\sigma_0/J=30$ to $b\sigma_0/J\approx3$ at the LSY loading of $b\sigma_0/J=30$. Again, the zone of

$J-A_2-M$ dominance is larger than that of $J-A_2$ dominance for the high hardening material, and the $J-A_2-M$ solution should be used to describe the crack-tip field for the bending specimen under LSY conditions.

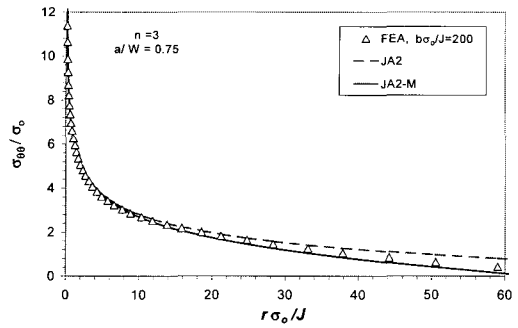

(a)

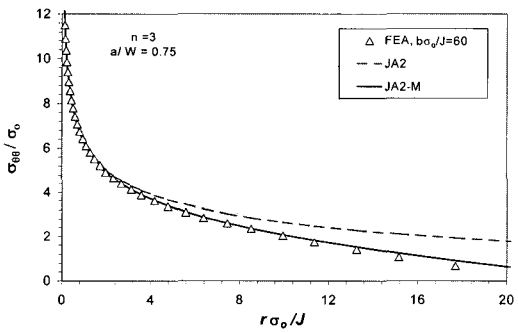

(b)

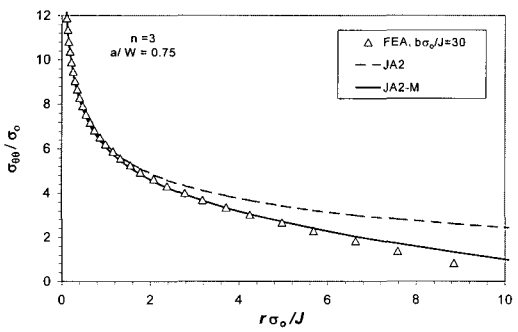

(c)

Fig. 4 Distribution of the opening stress along the ligament from FEA results and the asymptotic solution for the specimen with a/W=0.75 and n=3 (a)$b\sigma_o/J=200$, (b)$b\sigma_o/J=60$, (c)$b\sigma_o/J=30$

5. Conclusions

A simple modification of the $J-A_2$ solution was developed in this work to address the influence of the global bending on the crack-tip field for bending dominated specimens under LSY conditions. The detailed plane strain FEA calculations were then performed for the SENB with a deep crack of a/W=0.75 for two hardening exponents under different loading levels from LSY to SSY to demonstrate the effect of the global bending on crack-tip stress fields. The primary results are summarized as follows:

(1) The $J-A_2$ three-term solution is only a good approximation of the crack-tip fields up to the contained yielding conditions or $b\sigma_0/J\approx 60$ for bending specimens.

(2) The global bending stress dominates the crack-tip field for bending specimens, and the global bending influence is significant under LSY conditions or $b\sigma_0/J\leq 30$.

(3) The crack-opening stress is a linear function of the normalized distance, $r/(J/\sigma_0)$ under LSY conditions.

(4) The modified $J-A_2$ four-term solution still only contains the two parameters, i.e. $J$and A_2, without introducing any new parameter. Comparison with FEA results show that it can effectively characterize the crack-tip field of bending specimens under LSY conditions beyond capability of the conventional $J-A_2$ solution.

(5) The parameter A_2 can be determined by Eq. (6) to accurately quantify the

constraint levels at the crack tip of bending specimens under LSY conditions.

It is noted that the proposed solution was only validated by FEA for the A533B steel considered. Further FEA validations are needed for other ductile materials so that the modified $J-A_2$ solution proposed in this work can be used as a viable tool to characterize the crack-tip field and quantify the crack-tip constraint for bending dominate geometries in practical defect assessment of engineering structures.

Acknowledgments

The first author acknowledges the support to this work from Mokpo National Maritime University.

References

[1] Rice, J. R., A path independent integral and the approximate analysis of strain concentration by notches and cracks, Journal of Applied Mechanics, 35: 379-386, 1968.

[2] Hutchinson, J. W., Singular behavior at the end of a tensile crack in a hardening material, Journal of the Mechanics of Physics and Solids, 16: 13-31, 1968.

[3] Rice, J.R. and Rosengren, G.F., Plane strain deformation near a crack tip in a power law hardening material, Journal of the Mechanics of Physics and Solids, 16: 1-12, 1968.

[4] Jang, S.K. and Zhu, X.K., Two-parameter characterization for the resistance curves of ductile crack growth, Journal of the Korean Society of Marine Engineers, 23: 70-85, 1999.

[5] Zhu, X. K. and Jang, S. K., J-R curves corrected by load independent constraint parameter in ductile crack growth, Engineering Fracture Mechanics, 68: 285-301, 2001.

[6] Zhu, X.K. and Chao, Y.J., Constraint effects on crack-tip fields in elastic-perfectly plastic materials, Journal of the Mechanics and Physics of Solids, 49: 363-399, 2001.

[7] Betegon, C. and Hancock, J.W., Two parameter characterization of elastic-plastic crack-tip fields, Journal of Applied Mechanics, 58: 104-110, 1991.

[8] Al-Ani, A. M. and Hancock, S. W., J-dominance of short cracks in tension and bending, Journal of the Mechanics of Physics and Solids, 39: 23-43, 1991.

[9] O'Dowd, N. P. and Shih, C.F., Family of crack-tip fields characterized by a triaxiality parameter I. structure of fields, Journal of the Mechanics of Physics and Solids, 39: 989-1015, 1991.

[10] O'Dowd, N.P. and Shih, C.F., Family of crack-tip fields characterized by a triaxiality parameter II. fracture applications, Journal of the Mechanics of Physics and Solids, 40: 939-963, 1992.

[11] Yang, S., Chao, Y. J. and Sutton, M. A., Higher-order asymptotic fields in a power-law hardening material, Engineering Fracture Mechanics, 45: 1-20, 1993.

[12] Chao, Y. J., Yang, S. and Sutton, M.

A., On the fracture of solids characterized by one or two parameters: theory and practice, Journal of the Mechanics of Physics and Solids, 42: 629-647, 1994.

[13] Chao, Y. J. and Zhu, X. K., J-A2 characterization of crack-tip fields: extent of J-A2 dominance and size requirements, International Journal of Fracture, 89: 285-307, 1998.

[14] Shih, C. F. and German, M. D., Requirements for a one parameter characterization of crack tip fields by HRR singularity, International Journal of Fracture, 17: 27-43, 1981.

[15] Parks, D. M.,, Advances in characterization of elastic-plastic crack-tip fields, Fracture and Fatigue, A.S. Argon, Ed., Spring-Verlag, New York, 59-98, 1992.

[16] Wang, Y. Y. and Parks, D. M.,, Limit of J-T characterization of elastic- Plastic Crack-Tip Fields, Constraint Effects in Fracture Theory and Applications: Second Volume, ASTM STP 1244, Mark Kirk and Ad Bakker, Eds., American Society for Testing and Materials, Philadelphia, 43-67, 1995.

[17] Wei, Y. and Wang, T., Characterization of elastic-plastic fields near stationary crack tip and fracture criterion, Engineering Fracture Mechanics, 51: 541-553, 1995.

[18] Karstensen, A.D., Nekkal, A. and Hancock, J.W., Constraint estimation for edge cracked bending bars, IUTAM Symposium on Nonlinear Analysis of Fracture(J.R. Willis ed.), Kluwer Academic Publishers, Netherlands, 23-32, 1997.

[19] Lam, P. S, Chao, Y. J., Zhu, X. K., Kim, Y., and Sindelar, R. L., Determination of constraint-modified J-Rcurves for carbon steel storage tanks, Journal of Pressure Vessel Technology, 123: 111-222, 2003.

[20] Chao, Y.J. and Zhang, L., Tables of plane strain crack tip fields: HRR and higher order terms, Me-Report, 97-1, Department of Mechanical Engineering, University of South Carolina, 1997.

Author Profile

Seok-Ki Jang

Professor, Dept. of Marine System Engineering, Mokpo Maritime University. Ph.D. in Mechanical Engineering, Channam National University, 1988.

Xianqui Zhu Ph.D

Principal Research Scientiest
Battelle, Pipeline Technology Center
Columbus, OH43201, U.S.A.